J Mater Sci (2008) 43:1638–1643
DOI 10.1007/s10853-007-2347-6

Low temperature synthesis of nanocrystalline Sb_2Te_3 by mechanical alloying

M. Zakeri · M. Allahkarami · Gh. Kavei · A. Khanmohammadian · M. R. Rahimipour

Received: 8 July 2007 / Accepted: 27 November 2007 / Published online: 25 December 2007

Abstract $Sb_{40}Te_{60}$ thermoelectric compound was fabricated via mechanical milling of bismuth and tellurium as starting materials. Effects of the milling time and heat treatment were investigated. X-ray diffraction (XRD) was used for the characterization of the ball-milled powders. Thermal behavior of the mechanically alloyed powders was studied by differential thermal analysis (DTA) and the morphological evolutions were monitored by scanning electron microscopy (SEM). Results showed that the reaction between Sb and Te initiated after 5 h of milling and completed after 10 h. The synthesized Sb_2Te_3 had anisotropic property with the mean grain size of 13 nm at the end of milling. Also this compound could not be formed during heating by DTA at low temperatures (<500 °C). Under the sintering conditions the maximum values of electrical conductivity and power factor were found to be 860 $(\Omega\ cm)^{-1}$ and 45 $(\mu W\ cm^{-1}\ K^{-1})$, respectively.

Introduction

Thermoelectric devices are used in a variety of applications including military for night vision equipment, electronic equipment cooling, portable refrigerators, and inertial guidance systems [1]. Thermoelectric devices are advantageous due to their reliability, lightweight, small size, quietness, and reasonable price. They are also able to function in severe, sensitive, or small environments for conventional refrigeration. These environmentally adjustable devices offer precise temperature control, while requiring minimal maintenance because they have no moving parts. Thermoelectric devices are useful for small cooling jobs where a compressor based system would be impractical. These devices are also functional because they can heat as well as cool depending on the polarity of the power source [2]. There are several preparation methods for these materials. Unidirectional crystal growth by zone melting, e.g., traveling heating method (THM), is widely used. This method usually exhibits good thermoelectric properties; however long process time is needed and also the products have anisotropic and poor mechanical properties [3]. With the requirement of a good combination of thermoelectric and mechanical properties, powder metallurgy is extensively used for the preparation of thermoelectrics. Nevertheless, efficiency and contamination are two serious problems during this traditional powder metallurgical process [4].

Mechanical alloying is a powerful powder processing method, which had been used to synthesize various alloy powders with extremely fine microstructures. Mechanical alloying (MA) is basically a dry and high-energy ball milling process, which has been used for the synthesis of alloys, oxide-dispersion-strengthened alloys, amorphous alloys, various intermetallic compounds, and thermoelectric and magnetic materials [5–7].

Yang et al. [8, 9] prepared bismuth telluride-based *n*-type thermoelectric materials via mechanical alloying and subsequent hot pressing process. They investigated the influence of hot pressing parameters and Ag doping on the thermoelectric properties. They obtained a maximum figure

M. Zakeri (✉) · M. Allahkarami · Gh. Kavei · M. R. Rahimipour
Ceramic Department, Materials and Energy Research Center, Tehran, Iran
e-mail: m_zakeri@iau-saveh.ac.ir; M.Zakeri@iau-saveh.ac.ir

A. Khanmohammadian
Materials Engineering Department, Islamic Azad University (Saveh branch), Saveh, Iran

of merit of 1.7 × 10^{-3} $K^{-1}$for the 4 h hot pressed and 0.2 wt.% Ag. In the other researches, starting from element Bi, Se, Te, and Sb granules, thermoelectric materials with different compositions were prepared via mechanical alloying and hot pressing. They investigated the effect of chemical composition, doping content, and annealing on the thermoelectric properties and obtained optimum conditions [2, 10, 11]. In the Kim et al.'s study, the 20%Bi_2Te_3–80%Sb_2Te_3 alloy exhibited a maximum figure of merit of 3.05 × 10^{-3} K^{-1} [12]. Lopez et al. [13] synthesized the solid solution of Bi–Sb–Te by mechanical alloying. They exhibited very promising carrier concentration values for thermoelectric applications.

It should be noted that all of the above researchers investigated complicated compositions such as $(Bi_2Se_3)_x$ $(Bi_2Te_3)_{1-x}$ or Bi_2Te_3–Sb_2Te_3–Sb_2Te_3. It seems very interesting that Bi_2Te_3 or Sb_2Te_3 compounds have thermoelectric properties in the simple forms and can be used as thermoelectric materials. The synthesis of these compounds is also easier than other complicated compositions. Synthesis of these compounds by mechanical alloying led to the formation of nanostructured materials that improved thermoelectric properties.

The aim of this work is the synthesis of Sb_2Te_3 thermoelectric material by mechanical alloying. This is first time that this compound has been inexpensively prepared by this method in a short time process.

Experimental

Sb (99.999%, <1 mm) and Te (99.999%, <1 mm) were used as starting materials. These powders were mixed in stoichiometric Sb/Te ratio of 2/3 and subsequently charged into a stainless steel cup (125 mL) with the ball to powder weight ratio (BPR) of 10:1. High-chromium stainless steel balls were used in argon atmosphere with the pressure of 3 atm. The ball milling experiments were performed in a planetary ball mill at the cup and main disk speed of 275 and 525 rpm, respectively. Samples were removed by interrupting the ball mill at various intervals for analysis.

Phase transformation and crystallite size evolution during milling and heat treatment were studied by X-ray diffraction (XRD) analysis using a Philips (30 kV and 25 mA) diffractometer with Cu Kα radiation (λ = 1.5405 Å). All XRD experiments were performed with a step size of 0.02° and a time per step of 1 s. Crystallite size and lattice strain were evaluated using four different methods [14–16]. The morphology of the mechanically alloyed powder samples was examined by a Philips Scanning Electron Microscope (SEM) operating at 20 kV. Average particle size of milled samples was determined by SEM images (Diameter of approximately 300 particles randomly measured). To investigate the thermal behavior of the milled powders, differential thermal analyzer (DTA) was used. The samples were heated up to 500 °C with the heating rate of 10 °C/min under argon flow atmosphere.

The Sb_2Te_3 mechanically alloyed powder (25 h) was mixed with 5 wt.% Se and 0.03 wt.% Cd_2Cl as doping to prepare n-type semiconductor. Samples in a size of 4 × 4 × 20 mm were cold-pressed by hydraulic press under the pressure of 1 GPa and sintered in vacuum at the various temperatures of 450, 500, 550, and 600 °C as a function of time. Electrical conductivity was measured by the four-point probe method. The values of α (Seebeck coefficient) were obtained using $\alpha = (dV/dT)$-24 for *n*-type materials, where 24 is associated with the used thermocouples (AlCr–AlNi) [17].

Results and discussion

Figure 1 presents the XRD patterns of the as-received (mixed) and mechanically alloyed (MAed) $Sb_{40}Te_{60}$ for different milling times. Antimony and tellurium were mixed with the ratio of Sb/Te: 2/3 as the starting materials that were confirmed by X-ray diffraction patterns of the as-received samples. Ball milling of the starting materials led to the initiation of Sb_2Te_3 formation reaction. The Sb_2Te_3 peaks appeared after 5 h of milling while Sb and Te elements remained in the ball-milled composition. With increasing milling time to 10 h, all of remained elements transformed to Sb_2Te_3. The XRD pattern of 10-h milled powder shows a single-phase composition of Sb_2Te_3 that implies the completeness of the formation reaction of Sb_2Te_3. In order to study the stability of the synthesized phase, milling times increased to 15, 20, and 25 h. Results in Fig. 1 showed that no change had been occurred except

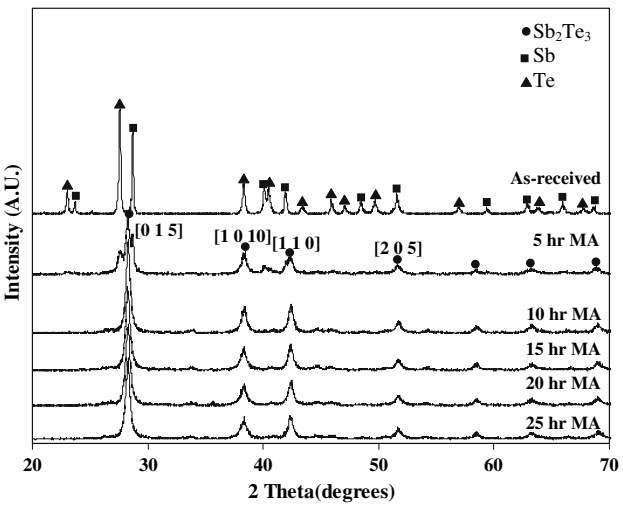

Fig. 1 X-ray diffraction patterns of as-received and ball-milled powders in different milling times

broadening of Sb_2Te_3 peaks that is due to the microstructure refinement (nanocrystalline grain formation and micro-strain induction by milling).

Each X-ray diffraction line profile obtained in a diffractometer is broadened due to instrumental and physical (crystallite size and lattice strains) factors [16]. Therefore, the first indispensable step preparatory to the calculation of crystallite size and lattice strain from the recorded XRD scan is the determination of the pure diffraction line profile for a given reflection, whose breadth depends solely on the physical factors [16]. This pure line profile is extracted by removing (deconvolution) the instrumental broadening factor from the experimental line profile. Only then the pure line profile can be used for calculating the crystallite size and lattice strain. The reference powder was the same antimony telluride powder that annealed at 400 °C for 3 h.

For comparative purposes the separation of crystallite size and strain broadening from the pure profile breadth was carried out by four methods. In the first one it was assumed that strain broadening and crystallite size were approximated Gaussian and Cauchy functions, respectively. The resulting equation for the crystallite size and strain is:

$$\frac{\delta^2(2\theta)}{\tan^2\theta_\circ} = \frac{K\lambda}{L}\left[\frac{\delta(2\theta)}{\tan\theta_\circ \sin\theta_\circ}\right] + 16e^2 \tag{1}$$

where δ is the pure line profile width at half maximum obtained by computer software Curve Expert 1.3 and Data Fit 8.2. $\theta_\circ$ is the position of the analyzed peak, λ the X-ray wavelength, L the crystallite size, and e the maximum strain. For all practical purposes the constant K can be set equal to unity [16]. Any available orders of a given reflection may be used to construct a linear plot of $\frac{\delta^2(2\theta)}{\tan^2\theta_\circ}$ versus $\frac{\delta(2\theta)}{\tan\theta_\circ \sin\theta_\circ}$. In the present work the [0 1 5], [1 0 10], [1 1 0], and [2 0 5] peaks were used. From the slope λ/L and ordinate intercept $16e^2$, the crystallite size, L, and strain, e, may be determined.

The second method was based on the assumption that the crystallite size and strain line profiles were both presumed to be Cauchy and the appropriate equation for the separation of crystallite size and strain is presented as the following [16]:

$$\delta(2\theta)\cos\theta_\circ = \frac{\lambda}{L} + 4e\sin\theta_\circ \tag{2}$$

Again, through plotting, the crystallite size can be attained from the intercept and the strain from the slope. Equation 2 was first proposed by Williamson and Hall [14] and is customarily referred to as the Williamson–Hall method.

The third method is quite similar to the second one, but now the size and strain line profiles are both presumed to be Gaussian and the appropriate equation takes the following form [16]:

$$\delta^2(2\theta)\cos^2\theta_\circ = \left(\frac{\lambda}{L}\right)^2 + 16e^2\sin^2\theta_\circ \tag{3}$$

As before, one can get both L, and e, from a linear plot.

The fourth method is similar to the second method with same equation, but now the size and strain line profile are both presumed to be Gaussian.

All of the above calculations were performed on the four mentioned (indexed in Fig. 1) peaks. These calculations were unsuccessful for all of the four methods. Examples from each method are shown in Fig. 2. As seen, in most cases a substantial scatter of data points resulted without any chance of fitting a straight line (isotropic case) and sometimes the intercept resulting from the slopes was negative that is meaningless for the calculation of grain size.

For more clarity, it must be mentioned that the crystallite size, L, calculated from the mentioned methods is the volume-average of the crystallite dimension perpendicular to the diffracting planes (h k l) from which it is calculated. These results indicate that Sb_2Te_3 has anisotropic property. Therefore, the four used methods cannot be applied. For gaining the mean crystalline size the well-known Scherrer method was employed. In this method, it is assumed that the broadening is due to the very fine grains and the effect of the lattice strain is not taken into account; therefore the results have some inaccuracy.

$$L = \frac{0.9\lambda}{\delta(2\theta)\cos\theta_\circ} \tag{4}$$

In the present work the mean grain size was calculated in four diffraction planes with two fitting models of Cauchy and Gaussian. Then the average of these diffracting planes and two fitting models were presented in Table 1. As interestingly seen, in all diffracting planes, the mean crystalline size decreased as the milling time increased in both models. Also the average of the each model and total average had the same manner as the diffracting planes. The other interesting result of this table is that the average grain size calculated by Cauchy model is greater than the one from Gaussian model.

Differential thermal analyzing (DTA) curves of the as-received (as-mixed) and MAed $Sb_{40}Te_{60}$ powders are presented in Fig. 3. In both as-received and 5-h milled powders one endothermic peak is situated at 422 °C corresponding to the melting of tellurium [18]. Antimony and antimony telluride did not appear because of their higher melting point (904 and 892 K, respectively). This endothermic peak at 5-h milled sample is smaller than the as-received. This is confirmed by XRD results that show partial reaction between antimony and tellurium. The

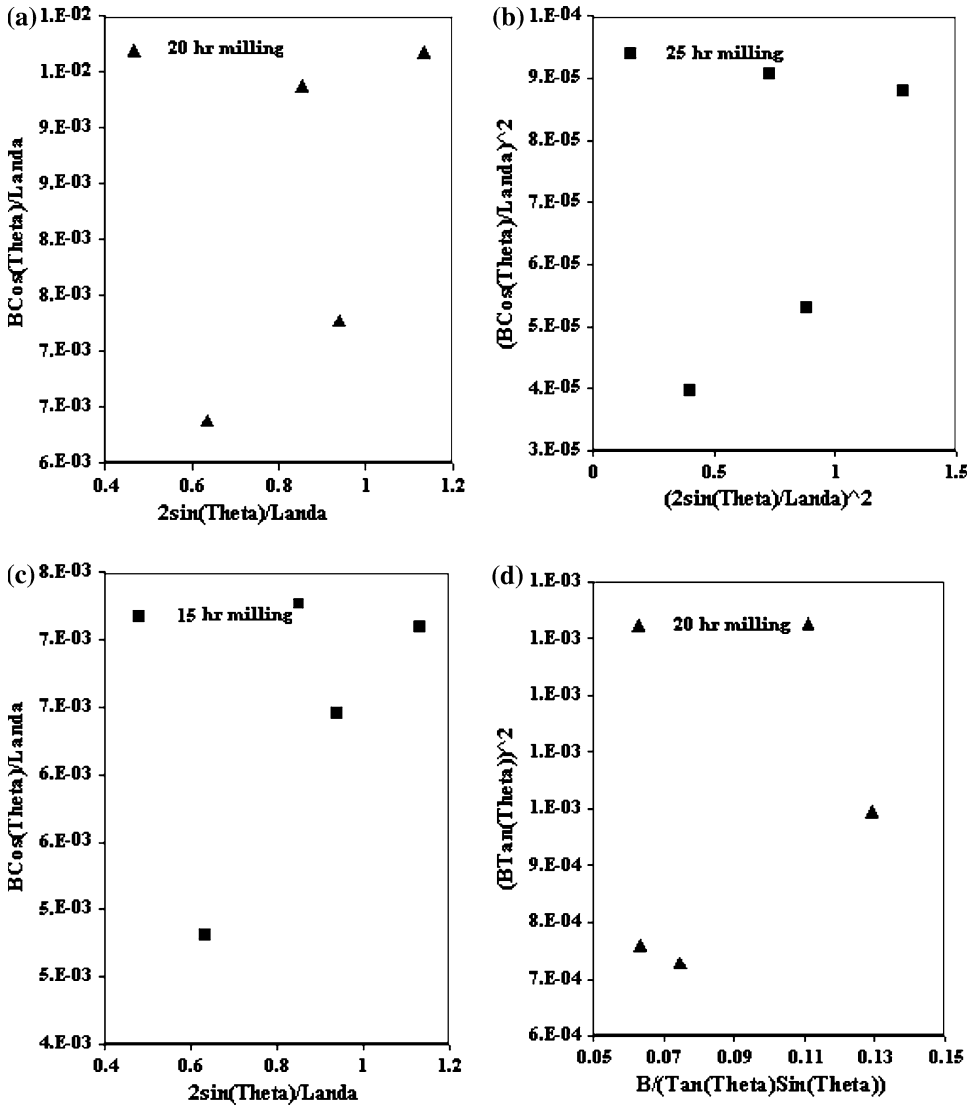

Fig. 2 Grain size and lattice strain separation with different methods: (**a**) Gaussian/Gaussian fitting with Eq. 2, (**b**) Gaussian/Gaussian fitting with Eq. 3, (**c**) Cauchy/Gaussian fitting with Eq. 1, and (**d**) Cauchy/Cauchy fitting with Eq. 2

Table 1 Grain size calculation by Scherrer method with two fitting models

Milling time (h)	Mean grain size (nm)										Total average
	Gaussian model					Cauchy model					
	[0 1 5]	[1 0 10]	[1 1 0]	[2 0 5]	Av.	[0 1 5]	[1 0 10]	[1 1 0]	[2 0 5]	Av.	
10	15.8	14.8	13.9	10.6	13.8	20.0	14.5	16.3	13.1	16.0	14.95
15	14.8	12.8	12.3	10.3	12.6	18.7	12.4	13.9	12.7	14.4	13.5
20	14.1	9.6	12.4	9.3	11.3	18.0	11.6	14.2	11.5	13.8	12.55
25	14.3	9.5	12.3	9.6	11.4	17.8	11.0	14.1	12.5	13.9	12.65

results indicate that Sb_2Te_3 cannot be formed by direct reaction during heating in both as-mixed and 5-h milled samples. Also it is implied that mechanical alloying is a very powerful method for synthesizing new materials at room temperature without heating.

Figure 4a shows the particle size distribution and morphology of the 5-h milled powder. It can be seen that powders had a wide range of size with very uneven large to very fine (submicron) particles. It is clear that fine particles adhered with weak forces to large particles. And the large agglomerates that are shown in Fig. 4b included very fine particles cold worked together strongly. In this stage of milling, cold working is major mechanism. With increasing the milling time to 15 h, cold working led to work

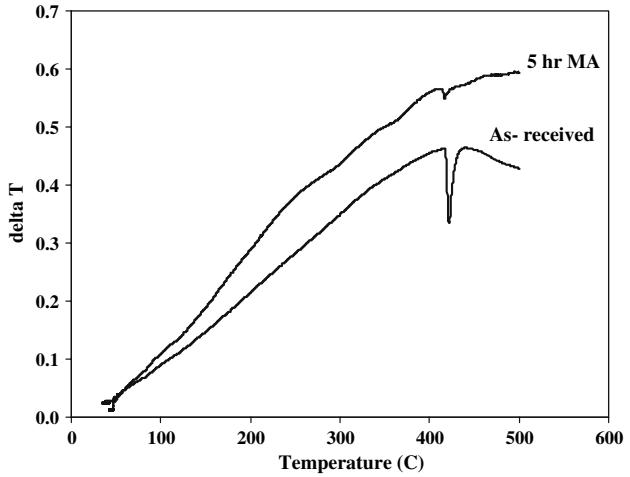

Fig. 3 DTA curves of the as-received and 5-h ball-milled powders for thermal behavior investigation

hardening and fracturing of particles. As a result, the average size and irregularity of particles decreased and also the distribution of particles was narrower (Fig. 4c). The other result of increasing the milling time was the modification of microstructure that is shown in Fig. 4d. It can be seen that the cold-worked particles were at submicron range (approximately 200–500 nm) but with a wide range of distribution. With further milling to 25 h no change occurred in the powder morphology and was very similar to 15-h milled powders (Fig. 4e). However, it can be seen in Fig. 4f that the powders had very fine microstructure (nanometer range <100 nm) with very narrow size distribution of cold-worked particles. Average particles size of milled powder after 25 h of milling was about 6.5μm.

Figure 5a shows the electrical conductivity (σ) variation of the hot-pressed samples at different temperatures and sintering times. It is obvious that sintering at all temperatures had the same results and behavior approximately. The electrical conductivity increased through the increase in the sintering time and reached a maximum of 860 $(\Omega\ \text{cm})^{-1}$ after 120 min of sintering at 550 °C. Further time for sintering led to the decrease in electrical conductivity. The power factor variation with sintering time and temperature

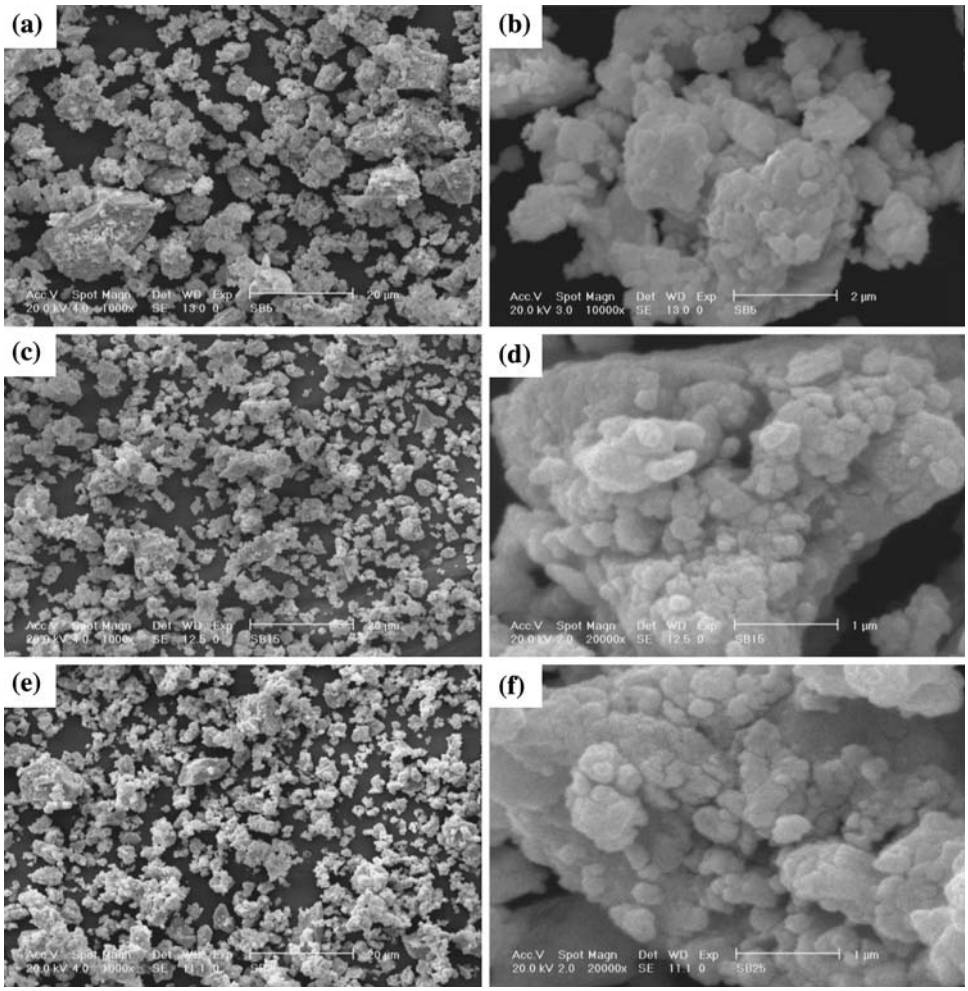

Fig. 4 Morphological and microstructural evolutions during milling via scanning electron microscopy (SEM): (**a**) 5-h milled, (**b**) cold-worked particles after 5 h of milling at higher magnification, (**c**) 15-h milled, (**d**) very fine microstructure of 15-h milled at higher magnification, (**e**) 25-h milled and (**f**) nanostructure of 25-h milled powder at higher magnification

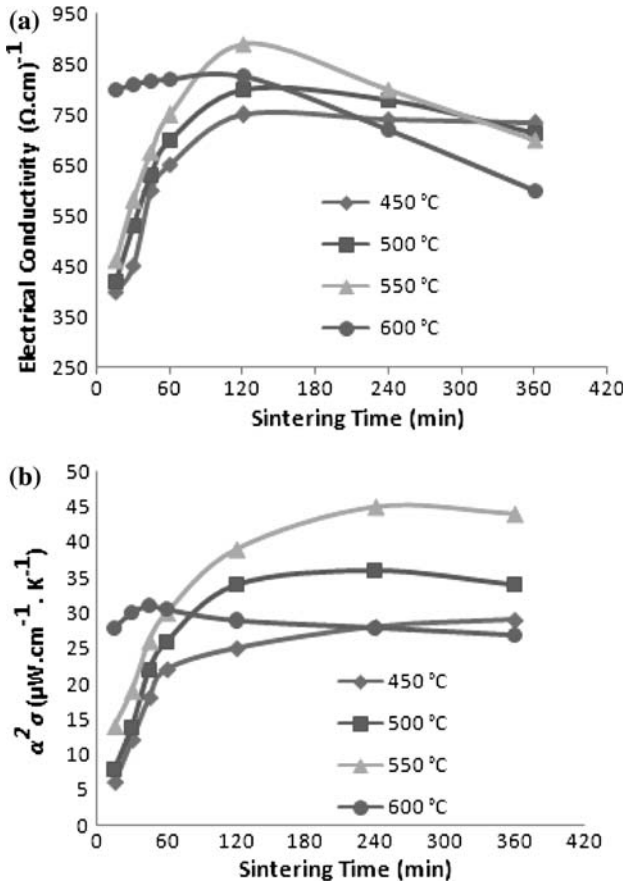

Fig. 5 (**a**) Electrical conductivity (σ) and (**b**) power factor ($\alpha 2\sigma$) variation as a function of sintering time and temperature

is shown in Fig. 5b. It can be seen that with increasing sintering time, the power factor increased and reached a constant value at each temperature. It is very interesting that the maximum value of power factor was obtained at 550 °C. These results indicate the best condition for sintering is 550 °C for 120 min. It should be noted that with increasing sintering temperature to 550 °C, the power factor increased, but further increase in sintering temperature to 600 °C led to the decrease in this factor.

Conclusion

Sb_2Te_3 as a new thermoelectric compound was synthesized by dry milling of elemental Sb and Te powder at room temperature. Nanocrystalline Sb_2Te_3 with the mean grain size of 13 nm was formed after 25 h of milling. The reaction between Sb and Te initiated at 5 h of milling and completed after 10 h of milling. Results indicated that the Sb_2Te_3 had anisotropic property, thus the conventional methods for measuring the grain size and lattice strain by XRD profiles can not be used. Heating the as-received and 5-h milled powders at DTA showed that Sb_2Te_3 could not be formed at low temperature (<500 °C). The best condition for sintering was 550 °C for 120 min. In these conditions the maximum value of electrical conductivity and power factor were 860 $(\Omega\ \text{cm})^{-1}$ and 45 (μW cm^{-1} K^{-1}), respectively.

References

1. Scherrer H, Chitroub M, Roche C, Scherrer S (1998) Proceeding of the International Conference on Thermoelectric, ICT, IEEE, Piscataway, NJ, USA, pp 115–120
2. Yang J, Aizawa T, Yamamoto A, Ohta T (2000) J Alloys Compd 309:225
3. Lennoir B, Dauscher A, Cssart M, Ravich Y, Scherrer H (1998) J Phys Chem Solids 59(1):129
4. Dzhafarov EG, Alieva TD, Abdinov D (2001) Inorg Mater 37(2):135
5. Syrayanarayana C (2001) Prog Mater Sci 46:1
6. Eskandarany El, Sherif M (2001) Mechanical alloying for fabrication of advanced engineering materials. Noyes Publication, Norwich
7. Zakeri M, Yazdani-Rad R, Enayati MH, Rahimipoor MR (2006) Mater Sci Eng A 430:185
8. Yang J, Fan XA, Ghen RG, Zhu W, Bao SQ, Duan X (2006) J Alloys Compd 416:270
9. Yang J, Chen R, Fan X, Bao S, Zhu W (2006) J Alloys Compd 407:330
10. Yang J, Aizawa T, Yamamoto A, Ohta T (2000) J Alloys Compd 312:326
11. Yang J, Aizawa T, Yamamoto A, Ohta T (2001) Mater Chem Phys 70:90
12. Kim HC, Oh TS, Hyun DB (2000) J Phys Chem Solids 61:743
13. Lopez RM, Lenoir B, Dauscher A, Scherrer H, Scherrer S (1998) Solid State Commun 108:285
14. Williamson GK, Hall WH (1953) Acta Metall 1:22
15. Zakeri M, Yazdani-Rad R, Enayati MH, Rahimipour MR, Mobasherpour I (2007) J Alloys Compd 430:170
16. Klug HP, Alexander L (1974) X-ray diffraction procedures for polycrystalline and amorphous materials, 2nd edn, chapter 9. John Wiley & Sons, New York, p 618
17. Petrov AV, Kutasov VA (1964) Thermoelectric properties of semiconductors, 1st edn. Springer
18. Kubaschewski O (1993) Materials thermochemistry, 6th edn. Oxford Pergamon Press